ISSN 2229-5518

Finite Element Analysis of Pressure Vessels and Joints using FEAST^{SMT}/PreWin and NISA/DISPLAYIII

BenilaVaghese, M.K.Sundaresan, Mathews.M.Paul

Abstract—Solid Rocket Motors (SRM) serve as the propulsion back-bone for strategic and tactical missiles as well as satellite launch vehicles. Motor case joints are mainly designed in SRM to prevent hot gas leakage and to reduce gap opening moments, the analysis of which can be incorporated with good accuracy using Finite Element Method (FEM). The flanged joint, segment joint and end dome to igniter joints are some of the important joints which are analysed to obtain its structural behavior. Estimation of stress in bolt under prestress, the structural deformations, the sealing of the O-ring to prevent the hot gas in segment joints and maximum stresses in joints and the walls is done using software FEASTSMT/PreWin (Finite Element Analysis of Structures). FEAST is ISRO's structural analysis software based on FEM realized by Structural Engineering entity of Vikram Sarabhai Space Centre (VSSC). The reliability of the software is established by comparing the analysis results of pressure vessel having different joint types with the results on another FEM software NISA/DISPLAYIII.

Index Terms—Motor case joints, structural behavior, gap, FEAST^{SMT}/PreWin, NISA/DISPLAY III.

1 Introduction

In satellite launch vehicles, SRM serve as the propulsion backbone. It constitutes the structural body of the rocket motor with its nozzle, propellant grain and so on and serves as a highly loaded pressure vessel. The cross section of a typical motor case is shown in Fig.1. Launch vehicle missions require larger l/d ratio for motor cases, which is made in number of segments. Hence metallic rings are used to join the segments in motor case, the design and development of which has become an important technology.

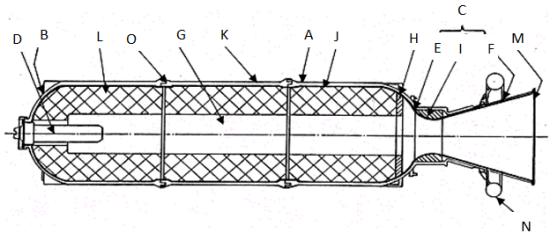

A	Chamber	I	Nozzle throat insert
B	Head end dome	J	Lining
C	Nozzle	K	Insulation
D	Igniter	L	Propellant
E	Nozzle convergent portion	M	Nozzle exit plane
F	Nozzle divergent portion	N	SITVC system
G	Port	O	Segment joint
H	Inhibitor		

Fig. 1. Cross-section of a typical rocket motor case [1]

Motor case subsystems such as nozzle and igniter are integrated through bolted flange joints. With different loading conditions, especially high loads, bolted connections can separate which can be minimized by the application of a pretension to the bolt. The link breakage of segment joint in the solid fuel rocket can lead to gas leakage and result in blast due to failure of the O-rings. Hence these connections are important to be analysed for the safe functioning of the system.

2 Objectives

From the literature survey [2], [3], [4], [5], [6], [7], [8], [9], [10] it is known that for the safe operation of the pressure vessel, estimation of stress in bolt under prestress, the structural deformations, the sealing of the O-ring to prevent the hot gas leakage in segment joints and maximum stresses in joints are to be estimated. FEAST is used for analysis and the software is to be validated by comparing the results of analysis with another finite element software.

3 Scope

- To model and do finite element analysis of pressure vessel with cylindrical shell, flanged joint, segment joint and end dome to end closure/igniter joint of SRM cases.
- Modelling is done using 2D axisymmetric elements.
- Structural analysis has been carried out for pressure loading.
- The analysis is done using FEASTSMT/PreWin and NISA / DISPLAY-III.

- ***Benila** Varghese is currently pursuing master of technology at Mar Athanasius College of Engineering,Kothamangalan. E-mail: benilavarghese2010@gmail.com*
- *M.K.Sundaresan is currentlyworking as a scientist in Vikram Sarabhai Space Centre, Trivandrum.*
- Mathews.M.Paul is currently the professor at Mar Athanasius College of Engineering, Kothamangalam.

- Comparison of results of analysis using both softwares.

4 Finite Element Analysis

4.1 Flanged Joint

To understand the joint behaviour, maraging steel cylinder pressure chamber of diameter 560 mm is considered. Geometry of the pressure chamber and flange are shown in Fig. 2. Different models of flanged joints by making different assumptions of stiffener effect are studied as below:

Case 1 - Bolted flanged joint
Case 2A- Flanged joint merged beyond Pitch Circle Diameter (PCD) with gap elements on interface
Case 2B - Flanged joint merged beyond PCD without gap elements on interface
Case 3 - Fully merged flanged joint (like stiffened cylinder)

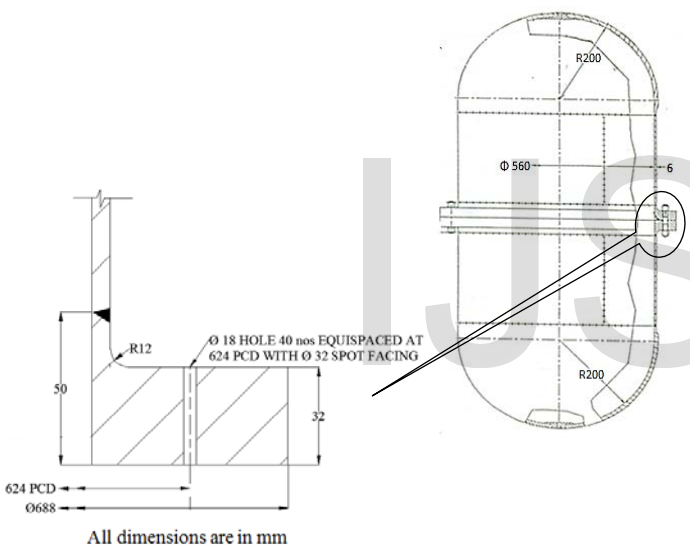

Fig. 2. Geometry of the pressure chamber

Material Properties

The material property of the pressure chamber and orthotropic property of bolt to simulate prestress is tabulated in Table 1 and Table 2 respectively.

TABLE 1
Material properties of the pressure chamber

PROPERTY	UNIT	VALUE
Ultimate tensile strength	N/mm²	1765.8
Yield strength	N/mm²	1726.6
Shear strength	N/mm²	1059.5
Young's Modulus	N/mm²	194238
Poisson's ratio	---	0.3

The model is idealized using 4-noded axi- symmetric element in NISA and FEAST as shown in Fig. 3. Interface is simulated using standard gap element between flanges, varying for different models as shown in Fig. 4. Internal pressure of 10 N/mm² is considered for the study. A pretension of 300 N/mm² is provided. The boundary condition of $U_Y = 0$ is provided at the free end of the cylindrical shell. Fasteners are simulated as axi-symmetric ring at the bolt PCD.

TABLE 2
Material properties of the bolt for simulation in bolt cylinder concept

PROPERTY		UNIT	VALUE
Young's Modulus	E_x	N/mm²	2.1
	E_y		210000
	E_z		2.1
Poisson's ratio	NUXY	----	$1x10^{-4}$
	NUYZ		$1x10^{-4}$
	NUXZ		$1x10^{-4}$
Coefficient of thermal expansion	α_x	\°c	1.2×10^{-15}
	α_y		1.2×10^{-5}
	α_z		1.2×10^{-15}

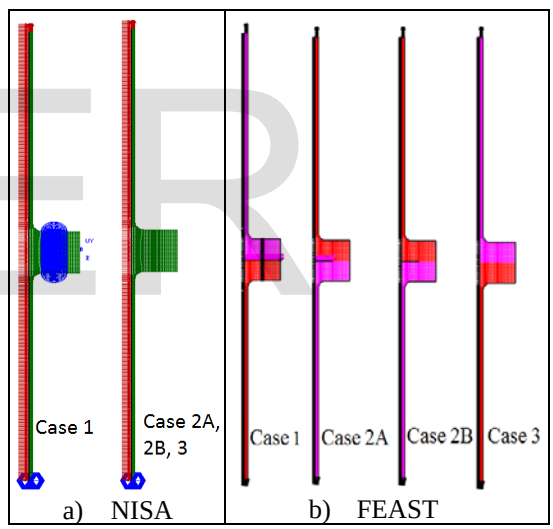

Fig. 3. FE model of pressure vessel with flange joint

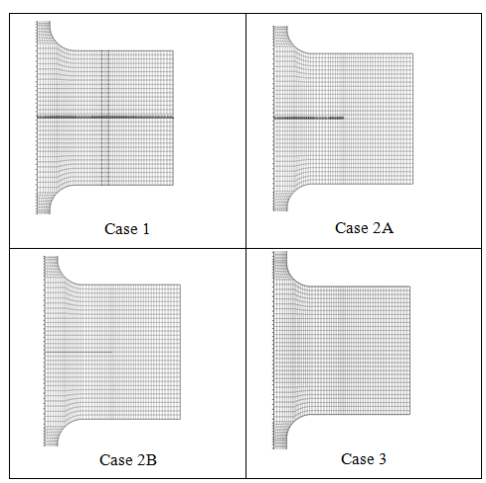

Fig. 4. FE model of flange portion

4.2 Segment Joint

The joint behavior is studied using maraging steel motor case. An internal pressure load of 6.47 N/mm² is applied. FE model of the segment joint is created with separate models of tongue and groove rings and are connected using the pin which is modeled by tying the nodes in Y-direction at the corresponding locations as shown in Fig. 5.

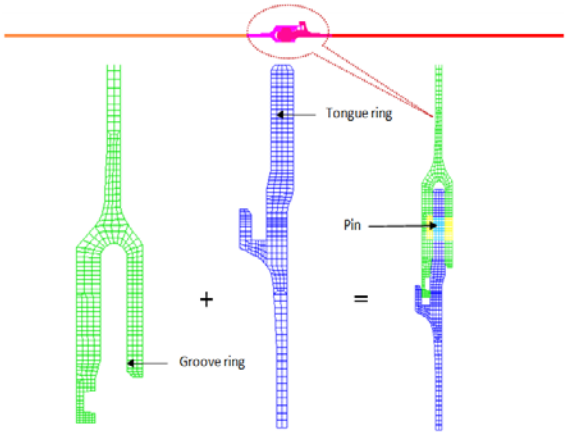

Fig. 5. FE model of parts of the segment joint

Modeling is done using 4-noded axi-symmetric elements as shown in Fig. 6. Gap elements are provided at the contact regions of tongue and groove portions. The boundary condition of $U_Y = 0$ is provided at the free end of the cylindrical shell.

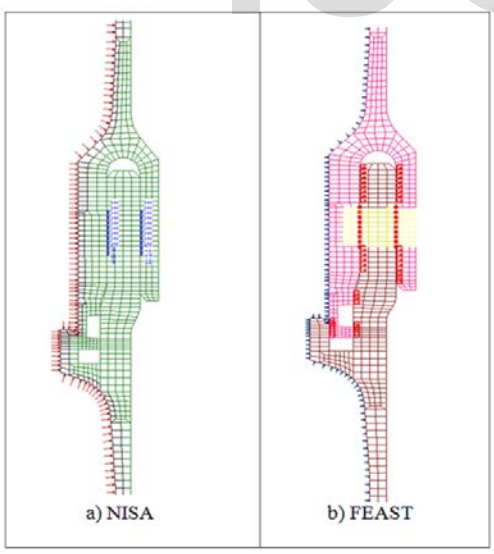

Fig. 6. FE model of the segment joint

4.3 Dome with End Closure

The material of fabrication considered here is M250 maraging steel**.** The end section is subjected to internal pressure loading of 6.47 N/mm². The end dome is connected to the end closure through flanged joint. Different models of the flanged portion by making different assumptions of stiffener effect are studied as below:

Case 1: Joint tied beyond PCD
Case 2: Joint merged beyond PCD

The FE model includes the end dome, the end ring and a portion of the cylindrical shell along with a flat plate closure at the fore end as shown in Fig. 7. The flanged joint is idealized with gap elements and tying varying in case 1 and 2 as shown in Fig. 8.

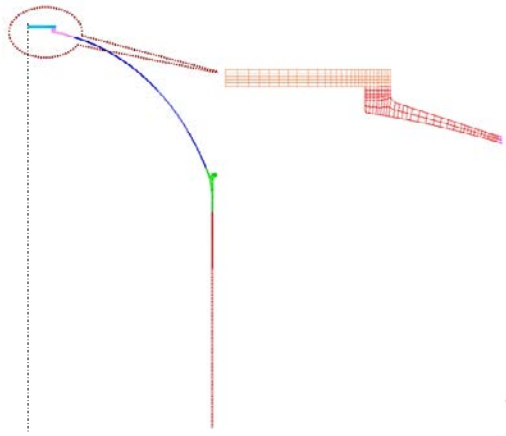

Fig. 7. FE model of dome with end closure

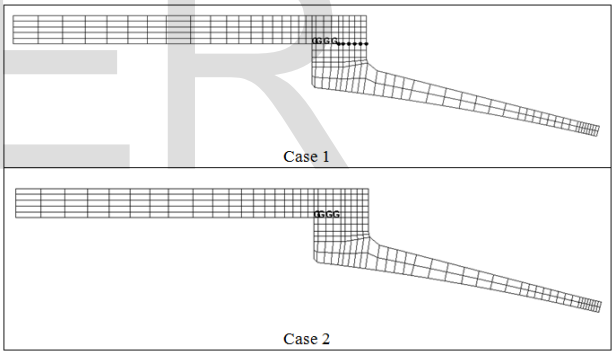

Fig. 8. FE idealisation of flange interface

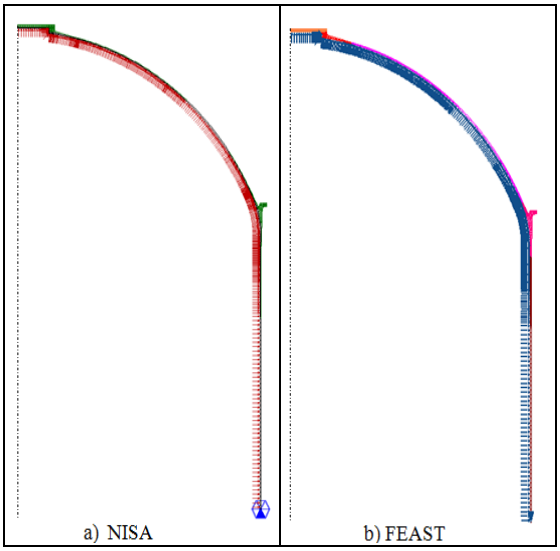

Fig. 9. FE model of end section

Modelling has been carried out using 2D axisymmetric 4-noded elements as shown in Fig. 9. The boundary condition of $U_Y = 0$ is provided at the free end of the cylindrical shell.

5 Results & Discussions

5.1 Flanged Joint

Stress Distribution

The model is validated and stress distribution for every section of the vessel and joint has been plotted using NISA and FEAST. The stress contours show similar pattern in both the softwares. The graph is plotted for longitudinal stress, hoop stress and von-Mises stress for each case at the positions shown in Fig. 10 using results from NISA and FEAST in Figures 11 to 19.

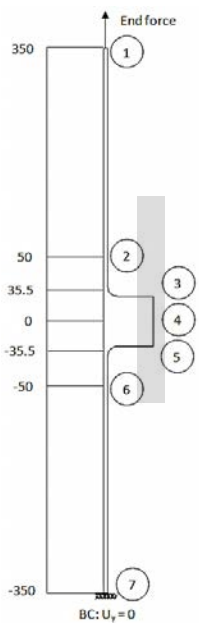

Fig. 10. Locations for stress determination in flanged jointmodel

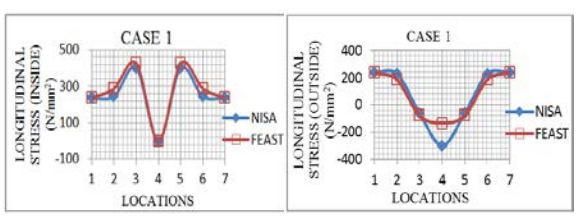

Fig. 11. Longitudinal stress-locations graph for case1

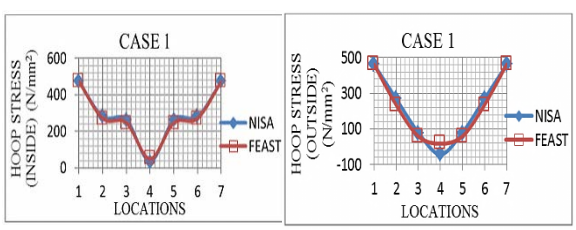

Fig. 12. Hoop stress-locations graph for case 1

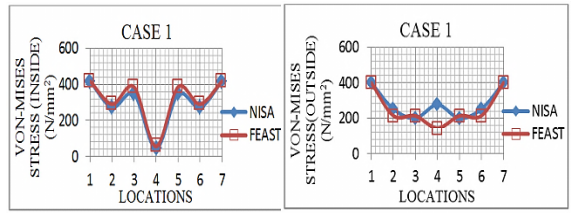

Fig. 13. von-Mises stress-locations graph for case 1

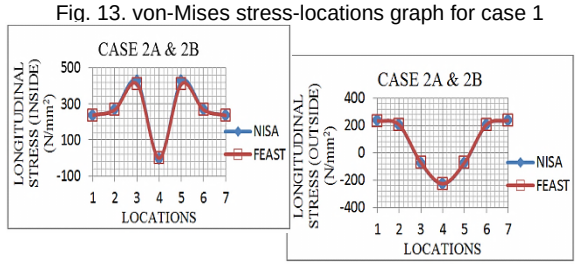

Fig. 14. Longitudinal stress-locations graph for case 2A & 2B

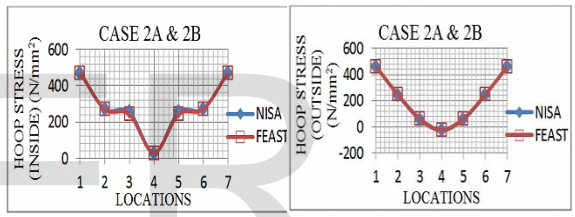

Fig. 15 Hoop stress-locations graph for case 2A &2B

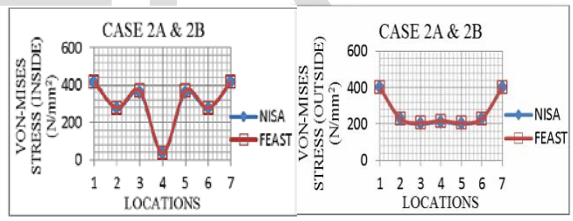

Fig. 16 von-Mises stress - locations graph for case 2A & 2B

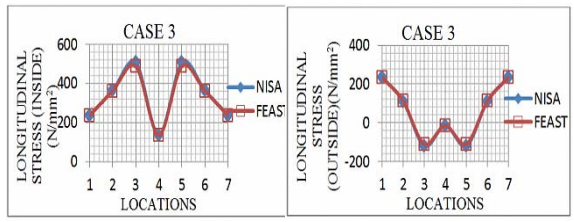

Fig. 17 Longitudinal stress-locations graph for case 3

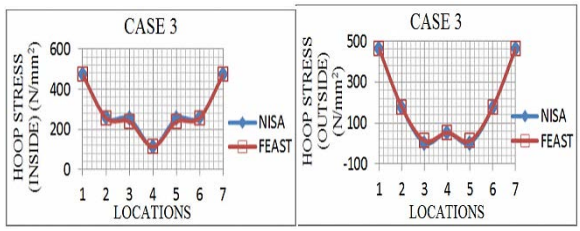

Fig. 18 Hoop stress-locations graph for case 3

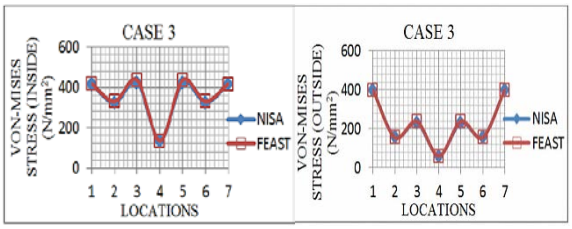

Fig. 19 von-Mises stress-locations graph for case 3

The graphs show that the results from both softwares are comparable. Case 2A and 2B has matching results showing that the presence of gap elements do not affect the analysis results for the configuration and loading considered. Also the stresses are within the yield strength of the material.

Deformation

The deformation characteristics for various cases in NISA and FEAST are as tabulated in Table 3 and the deformation pattern is shown in Figures 20 to 22. It can be seen that the results are comparable in both the softwares.

TABLE 3
Deformation results for flanged joint cases

DEFORMATION TYPE	CASE	NISA	FEAST
Radial deformation (mm) (at flange location)	1	0.06	0.076
	2A, 2B	0.049	0.049
	3	0.11	0.1
Overall deformation (mm)	1	0.873	0.839
	2A, 2B	0.833	0.834
	3	0.704	0.7046
Interface opening (mm)	1	0.308	0.21
	2A, 2B	0.249	0.251
	3	-NA-	-NA-
Axial growth (mm/m) (for the portion considered)	1	0.928	0.857
	2A, 2B	0.851	0.851
	3	0.564	0.564

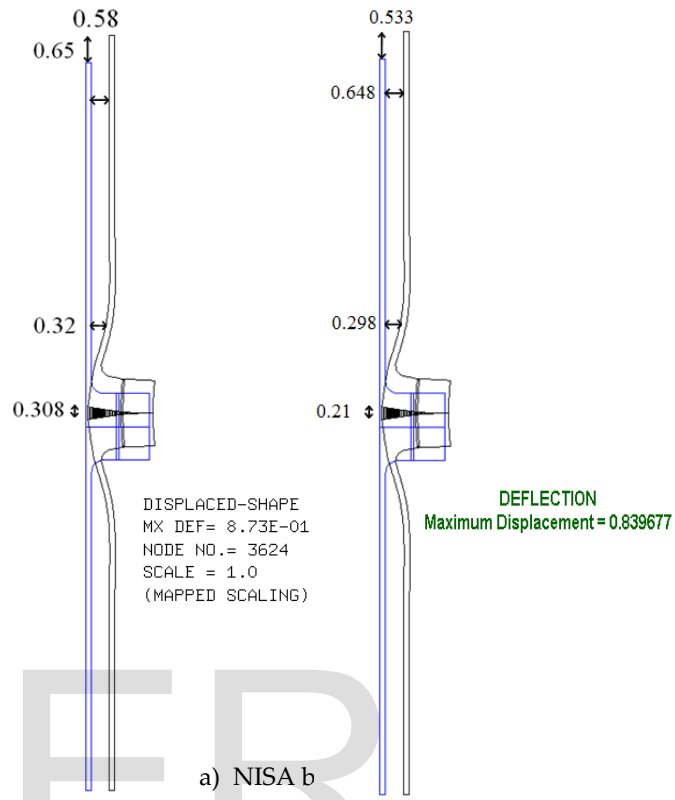

a) NISA b

Fig. 20.Deflected shape for case 1(mm)

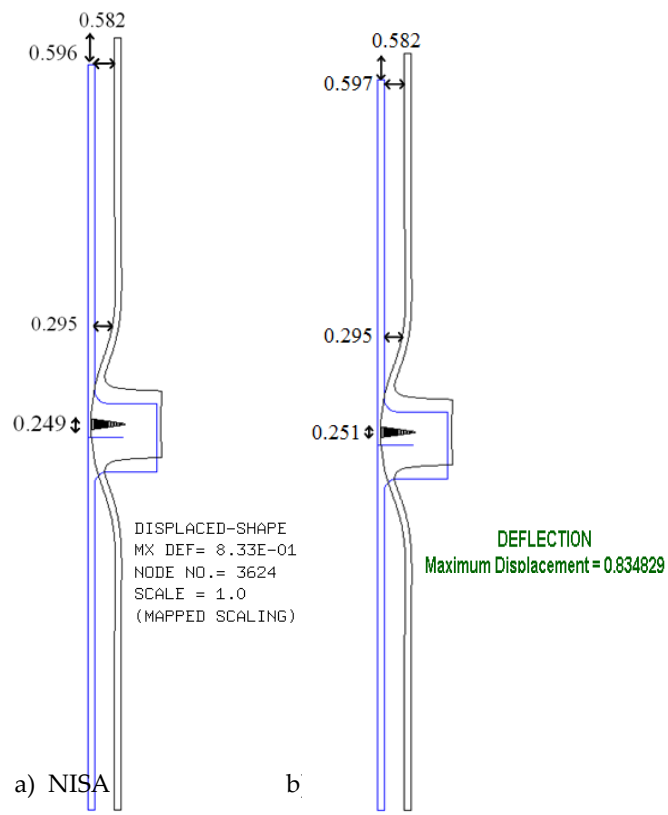

a) NISA b

Fig. 21. Deflected shape for case 2A & 2B (mm)

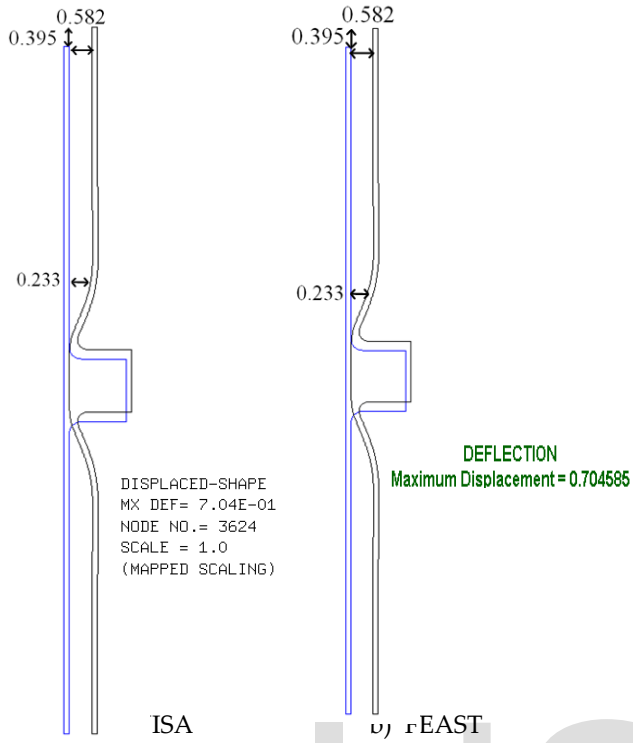

Fig. 22. Deflected shape for case 3 (mm)

Figures 23 to 25 depicts comparison between the results of gap element opening in the critical region of flange connection using both the softwares. It is observed that the deformation results from both the softwares is comparable.

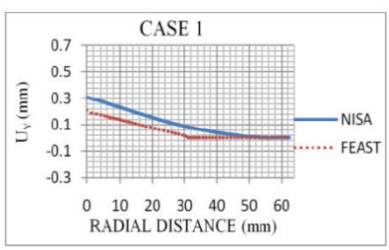

Fig. 23. Displacement-radial distance graph for case1

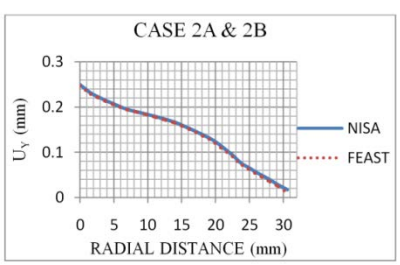

Fig. 24. Displacement-radial distance graph for case 2A& 2B

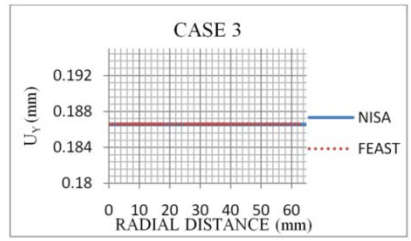

Fig. 25. Displacement-radial distance graph for case 3

5.2 Segment Joint

Stress Distribution

The stress results of cylindrical shell with segment joint from both the softwares at the locations shown in Fig. 26 is compared by plotting graphs as shown in Figures 27 to 29.

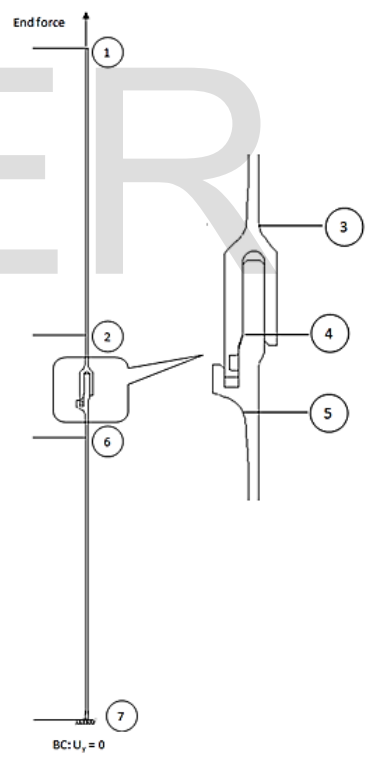

Fig. 26. Locations for stress determination in segment joint model

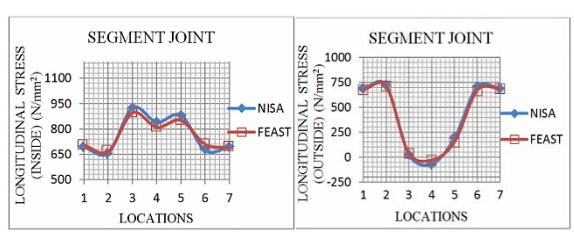

Fig. 27. Longitudinal stress-locations graph for segment joint model

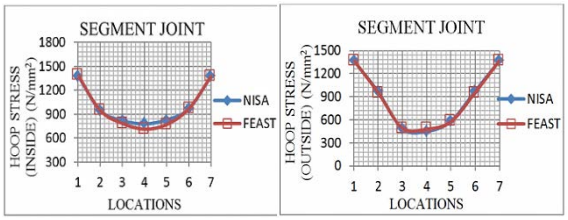

Fig. 28. Hoop stress-locations graph for segment joint model

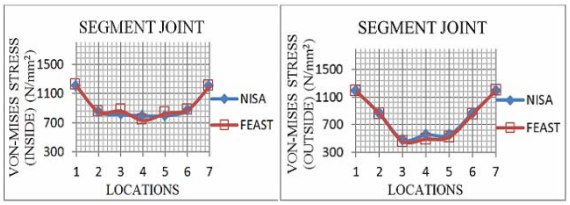

Fig. 29. von-Mises stress-location graph for segment joint model

From the graphs, it can be seen that the stresses are comparable in both the softwares at the locations considered. The stress contours is found to show similar pattern in both the softwares. All the stresses are within the yeild strength of the material.

Deformation

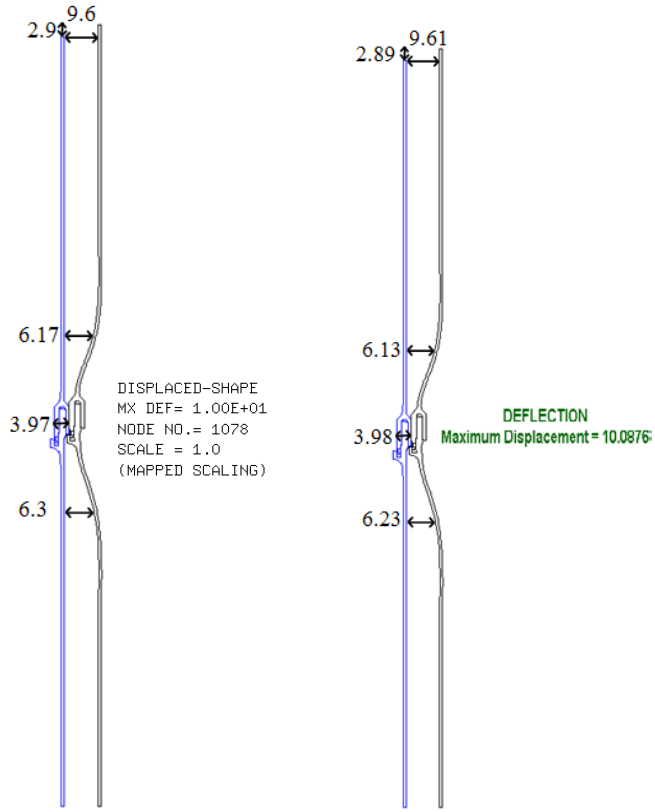

a) NISA b) FEAST

Fig. 30. Deflected shape of segment joint (mm)

Radial deformation, overall deformation and axial growth per unit length is observed as 3.97, 10 and 1.45 mm respectively in NISA. In FEAST, radial deformation, overall deformation and axial growth per unit length is found as 3.97, 10.087 and 1.45 mm respectively. At the position of weld near the joint, the deformations are 6.17 and 6.13 mm respectively in NISA and FEAST. The deformation pattern is shown in Fig. 30. The critical positions for the displacements are marked in the segment joint as shown in Fig. 31. The maximum deformation at positions 4, 5, 6 and 7 where O-ring is located is 1.32, 1.51, 1.51 and 1.48 mm respectively in NISA and 1.34, 1.49, 1.49 and 1.44 mm respectively in FEAST.

Fig. 31. Critical positions of segment joint

The graphs plotting deformation at the critical positions using both softwares is shown in Figures 32 to 38.

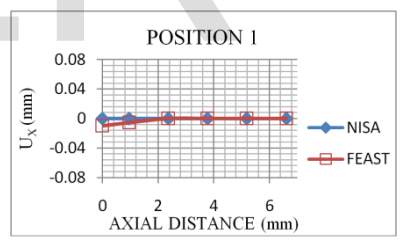

Fig. 32. Displacement-axial distance graph at position 1

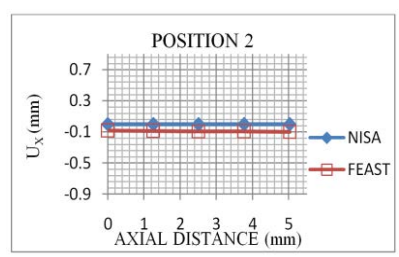

Fig. 33. Displacement-axial diatance graph at position 2

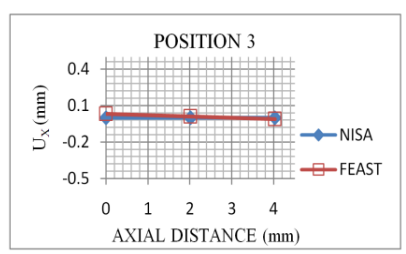

Fig. 34. Displacement-axial distance graph at position 3

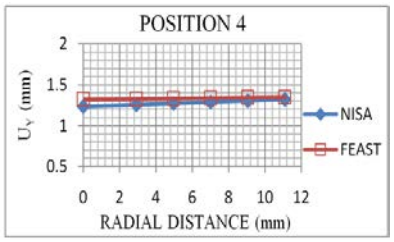

Fig. 35. Displacement-radial distance graph at position 4

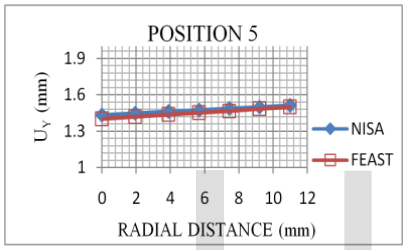

Fig. 36. Displacement-radial distance graph at position 5

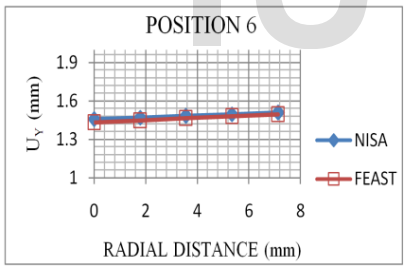

Fig. 37. Displacement-radial distance graph at position 6

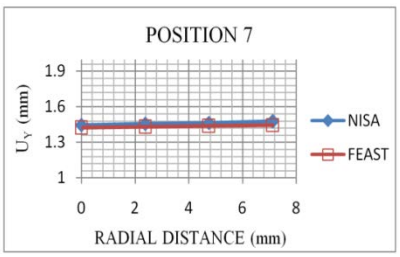

Fig. 38. Displacement-radial distance graph at position 7

It can be seen that the deformation values are comparing well in both the softwares.

5.3 Dome with End Closure

Stress Distribution

The longitudinal stress, hoop stress and von-Mises stress of the end dome section and the corresponding joint at the locations shown in Fig. 39 is graphically plotted in Figures 40 to 45.

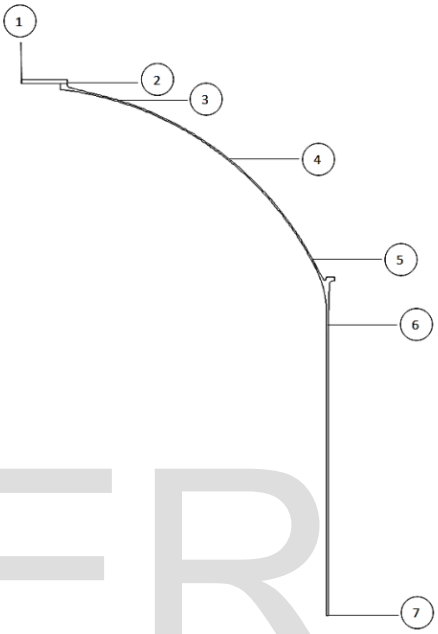

Fig. 39. Locations for stress determination in end dome section

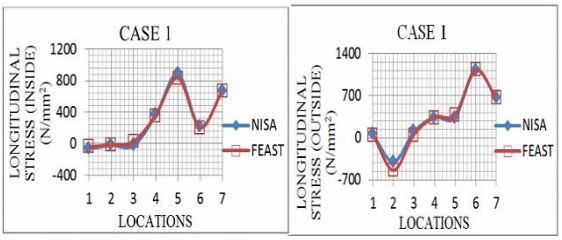

Fig. 40. Longitudinal stress-locations graph for case 1

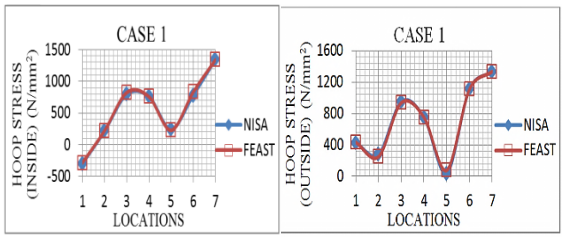

Fig. 41. Hoop stress-locations graph for case 1

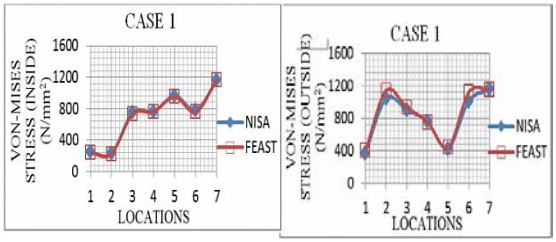

Fig. 42. von-Mises stress-locations graph for case 1

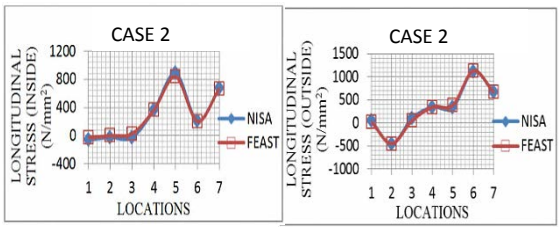

Fig. 43. Longitudinal stress-locations graph for case 2

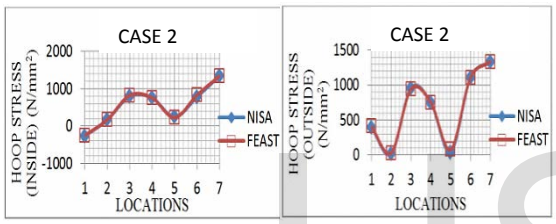

Fig. 44. Hoop stress-locations graph for case 2

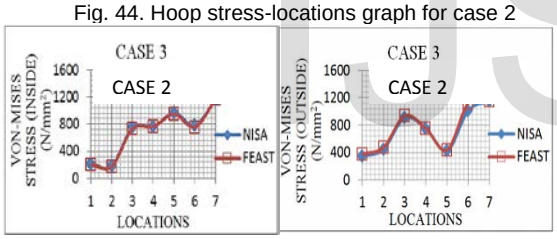

Fig. 45. von-Mises stress-locations graph for case 2

It can be seen that the stress results show comparable pattern. All the stresses are within the yield strength of the material.

Deformation

The radial deformation, overall deformation and interface opening for the models is tabulated in Table 4 and the deformation pattern is shown in Fig. 46.

TABLE 4
Deformation results for end section

DEFORMATION TYPE	CASE	NISA	FEAST
Radial deformation (mm)	1	9.36	9.36
	2	9.36	9.36
Overall deformation (mm)	1	9.96	9.99
	2	9.96	9.99
Interface opening (mm)	1	0.223	0.228
	2	0.223	0.228

It can be seen that the deformation results from both the softwares are comparable. At the region of the ring, the stiffness is improved and the deformation is less (2.07 and 2.08 mm respectively in NISA and FEAST) compared to the surrounding region. The deformation at weld region near the ring is 6.14 and 6.34 mm respectively in NISA and FEAST.

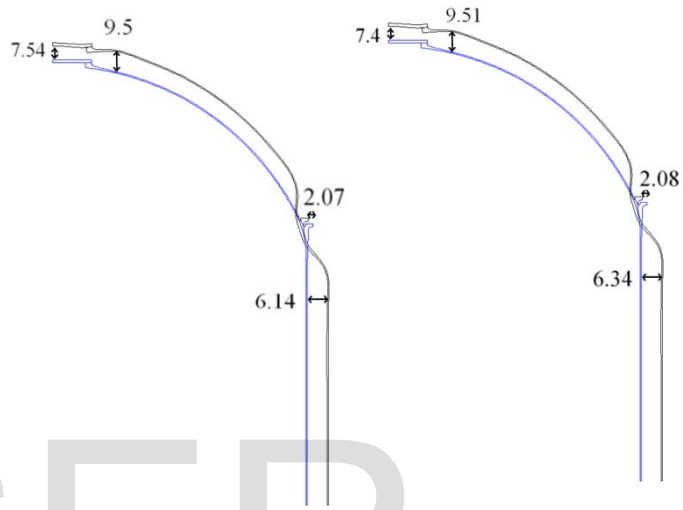

a) NISA b) FEAST

Fig. 46. Deflected shape of case 1and case 2 models(mm)

The comparative graphs showing deformation at the interface of the flanged connection for case 1and 2 in NISA and FEAST are shown in Figures 47 and 48.

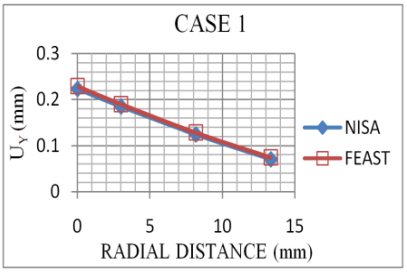

Fig. 47. Displacement-radial distance graph for case1

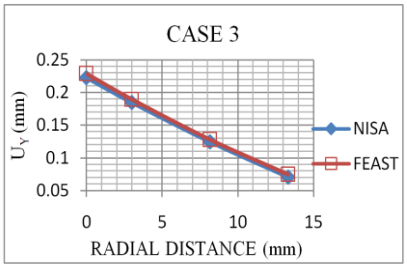

Fig. 48. Displacement-radial distance graph for case 3

Case 1 and 2 show similar results of deformation. The interface displacement is found to be comparable using both the softwares NISA and FEAST.

6 Conclusions

- In the analysis of the pressure vessel with cylindrical shell, flanged joint, segment joint and end dome to end closure/igniter joint of solid rocket motor cases, it is found that the stresses in the pressure vessel and joint are within the yield strength of the material.
- The cases with and without gap elements had similar results showing that the presence of gap elements doesn't affect the analysis results for the case considered.
- The results obtained using FEAST, in house software developed in VSSC, for all the models is found to compare well with those obtained using NISA.

References

[1] Krishnaveni.A and Christopher.T, *Probabilistic fracture mechanics studies in the reliable design of pressure vessels*, Shodhganga publications, March,2014.

[2] P. Rajamani , Dr. G .Srinivasa Gupta, *Design and Analysis of Rocket Motor Bolted Joint for Enhanced Strength*, International Journal of Innovative Research in Science, Engineering and Technology, Vol. 4, Issue 7, July 2015, pp.6396-6406.

[3] S. Mohammad Gharouni, Hamid M. Panahiha, JafarEskandari Jam, *Space shuttle Solid Rocket Motor (SRM) field joint: Review paper*, Association of Metallurgical Engineers of Serbia (AMES), October2014.

[5] Shivaji G. Chavan,*Stress Analysis of Flanged Joint Using Finite Element Method*, International Journal of Science and Research (IJSR), ISS 2319-7064,Volume 3 Issue 8, August 2014, pp.156-163.

[6] M.K.Sundaresan,G.Vinod, M. Manirajan , R. Suresh, C.K.Krishnadasan and B. Sivasubramonian, *Bolted Flanged Joint: Analysis and experimental evaluation*, Indian Conference on Applied Mechanics (INCAM), IIT Madras, 4-6 July 2013.

[7] Siva SankaraRaju R, Karun Kumar Y, Pragathi Kumar G, *Design and Analysis of Rocket Motor Casing by Using Fem Technique*, International Journal of Engineering and Advanced Technology (IJEAT), Volume-2, Issue-3, February 2013.

[8] V. Sivakumar and R. Palaninathan, *FE Analysis of Contact Pressure Prediction on O-Rings Used in Solid Rocket Booster Segment Joints*, International Journal of Science and Engineering Applications Volume 1, Issue.1, November 2012.

[9] BartlomiejZylinski and RyszardBuczkowski, *Analysis of Bolt Joint using the Finite Element Method*, The Archive of Mechanical Engineering, Vol. LVII, 2010.

[10] William H. Greene, Norman F. Knight, Jr.t and Alan E. Stockwell,*Structural behavior of the space shuttle SRM tang-clevis joint*, National Aeronautics and Space Administration (NASA), Hampton, September1986.